Photocatalytic oxidation of NO_x under visible light on asphalt pavement surface

Meng Chen[1], David.Baglee[2], Jiang Wei Chu[3] ,Dan feng Du[4],Xiu rong Guo[5]

[1]College of Traffic, Northeast Forestry University, 26 Hexing Road, Xiangfang District, Harbin, 150040, P.R. China, E-mail: chenmeng623@126.com

[2] Faculty of Applied Sciences, University of Sunderland, ST PETERS WAY, Sunderland, SR6 0DD, United Kingdom, E-mail: David.Baglee@sunderland.ac.uk

[3] College of Traffic, Northeast Forestry University, 26 Hexing Road, Xiangfang District, Harbin, 150040, P.R. China, E-mail: wildlife_deer@126.com

[4] College of Traffic, Northeast Forestry University, 26 Hexing Road, Xiangfang District, Harbin, 150040, P.R. China, E-mail: chenyuqi0831@163.com

[5] College of Mechanical and Electrical engineering, Northeast Forestry University, 26 Hexing Road, Xiangfang District, Harbin, 150040, P.R. China, E-mail: 785199452@qq.com

Corresponding author : Xiu rong Guo

Abstract:

This work examines the potential use of heterogeneous photocatalysis as an innovative oxidation technology. The aim is to demonstrate that this technology cand reduce the damaging effects of vehicle emissions by using nitrogen doped (N-doped) TiO_2 as a photocatalyst immobilized above the asphalt road surface. In the study, the photocatalytic effectiveness and durability of N-doped TiO_2 photocatalytic asphalt road material were assessed in both the laboratory and the field using direct and indirect measurement. The experimental results show that under visible light irradiation, N-doped TiO_2 asphalt road material has a higher activity compared with pure TiO_2 asphalt road material. The decontamination rate for NO_x is about 27.6%, 24.6%, 16.3%, and 13.8% under

irradiation at light wavelengths of 330–420 nm, 430–530 nm, 470–570 nm and 590–680 nm, respectively. Results of the field test and prediction models suggest that the service life of N-doped TiO_2 asphalt road material is approximately 13 months.

Key word: Photocatalyst; N-doping; visible light; Photocatalytic asphalt pavement; Nitrogen oxides

Introduction

Urban areas experience high levels of traffic exhaust, which contribute to air pollution, which is a major global concern (Ishihara et al. 2010). Many governments have introduced emission reduction systems in order to decrease emissions. In spite of these efforts, traffic has continued to increase, adding to concerns about the influence of traffic emissions on health and the environment. Researchers have found that asthma is associated with nitrogen oxide (NO_x), which pedestrians are exposed to due in part to the proximity of roads to walkways. Motor vehicle emissions must be decreased in order to reduce nitrogen oxide emissions, and thus reduce asthma rates (Tarek Mohamed et al. 2009). There are a number of methods that can be used to eliminate NO_x and other pollutants.

Recently, heterogeneous photocatalysis has emerged as an ecological technique for controlling air pollutants. In this technique, TiO_2 and pavement materials (such as cement and asphalt) are used together as a photocatalyst; this method has been found to be a promising and valid technology for NO_x control. The de-polluting properties of TiO_2 photocatalytic materials have been assessed by applying this method both in real-world use and in laboratory simulations

46 performed under different experimental conditions. Pone and Cheung (2006) evaluated the NO
47 removal paving blocks produced by waste materials and TiO_2. Their study included an optimum
48 mix design incorporating recycled sand, glass, 10% TiO_2, and cement achieved 4.01 $mgh^{-1}m^{-2}$ NO
49 removal. Husken et al., (2007) performed a comparative analysis of different photocatalytic
50 cementitious products in an optimum laboratory conditions. They found that the efficiency of NO_x
51 degradation varied significantly, with some products achieving 40% degradation while others had
52 no influence. In Bergamo, Italy in 2006 (Guerrini and Peccati. 2007) a 12,000 m^2 area, was
53 developed on the sidewalk and the road using active paving blocks. Environmental monitoring
54 showed an average NO_x abatement of 45% during the daytime (09:00 -- 17:00).
55 In asphalt roads, based on the porous characteristics of asphalt road materials, Meng Chen et
56 al. (2010) used permeability technology to apply asphalt nano-TiO_2 as an environmental
57 protection material. This test showed that this type of photochemical catalysis environmental
58 protection material had a purification function and the ability to protect the environment. Marwa
59 Hassan et al. (2013) used the pray method to make photocatalytic asphalt pavements. Laboratory
60 evaluation showed that the maximum NO_x removal efficiency was reached at an application rate
61 of 0.05 L/m^2. A research team in Italy used a mixed method approach to develop environmental
62 protection materials. TiO_2 was added into asphalt pavements as an apparent layer that is sprayed
63 onto existing pavements. The decrease in efficiency was dependent on the type of TiO_2
64 nanoparticles used, and the NO_x decrease efficiency ranged from 20–57% (Venturini et al. 2009).
65 Photocatalytic asphalt pavements mainly use anatase phase TiO_2. The TiO_2 band gap is 3.2eV,
66 which corresponds to wavelengths less than 388 nm. This limits the photocatalytic practice in the
67 UV light region, which amounts to 4% of the solar spectrum, while the key part (45%) falls under

the visible light region (Chun-Hung et al. 2010). Few studies have attempted to use photocatalytic asphalt pavements under visible light irradiation. Therefore, this study focuses on making a photocatalytic asphalt pavement material. As an innovative oxidation technology, it is able to reduce the damaging effects of vehicle emissions by using N-doped TiO_2 as a photocatalyst that is immobilized above the asphalt road's surface under visible light irradiation. The decontamination effect and application durability of the photocatalytic asphalt pavement material are also analyzed in this study.

Experimental

Photocatalysts preparation

A non-metal doping approach (N-doped TiO_2) was used to extend the utilization of the visible region in the solar spectrum. Titanium powder was prepared using a sol–gel approach that used tetrabutyl titanate (TNBT) and distilled water as the titanium precursor and hydrolyzing agent. First, TNBT was mixed with ethanol and distilled water. Then, the mixed solution was stirred using a machine under an 85℃ temperature bath for 6 hours. The slurry was dried at 80℃ and calcined at 400℃ for one hour. Finally, a white powder was obtained, which was pure TiO_2 (see Figure 1).

The pure TiO_2 powder was mixed with urea at molar ratios of 2:1, and then ground in an agate mortar for homogeneity. The mixed powders were heated in a muffle furnace at 500 °C for 3 h, resulting in N-doped TiO_2 (Figure 1).

Figure 1 shows that the N-doped sample appears yellow in color, compared to the white color of the pure TiO_2. Giacomo Barolo (2012) and Shinri Sato (1986) also observed these differences

in color and found that the yellow-colored N-TiO_2 had greater photocatalytic activity.

Preparation of asphalt road material through the addition of N-doped TiO_2 nanoparticles

We performed a series of penetrating load tests in order to attain a photocatalytic asphalt road material sample. First, based on our preliminary research (Meng and Yan hua. 2010), the penetrant and modified N-doped TiO_2 with silane coupling reagent were prepared. Then, the solution of mixed penetrant and modified N-doped TiO_2 was sprayed onto the bituminous sample's surface. In the load process, every sample was sprayed three times by an atmospheric air compressor. The caliber of the air compressor was 1.5mm and the air pressure was 3.0-3.5MPa. The samples were sprayed at a distance of approximately 20 cm and the speed of the aqueous solution jet was set at 8-10g/s.

Figure 2 and 3 display the schemes of the asphalt road material sample before and after spraying.

Analytical methods

Material property analytical methods

A scanning electron microscopy (SEM), and transmission electron microscopy (TEM) were used in this research in order to analyze the material properties of the N-doped TiO_2 and the photocatalytic asphalt road material. The SEM was a commercial Hitachi S2300 instrument with a tungsten hairpin filament. An accelerating voltage of 25 keV was used on gold samples to eliminate charging. Transmission electron microscopy analyses were performed using a JEM-2010 (JEOL) operating at 160 kV. T.

Photocatalytic degradation analytical methods

Direct and indirect measurement strategies were used in this research to evaluate the pollutant removal efficiency. Direct measurements were used in laboratory tests. In the laboratory test, 500 ppb of NO_x was put into the measurement system. After flowing through the photocatalytic asphalt road material, it was exported via the purification examination photoreactor of the system. Measurement results of the inlet and outlet of photoreactor show that the total NO_x concentration, the NO conversion, NO_2 conversion, and NO_x conversion were:

$$NO_x = NO + NO_2 \quad (1)$$

$$NO_{conversion} = \left(\frac{C_{NOin} - C_{NOlight}}{C_{NOin}} - \frac{C_{NObin} - C_{NOsb}}{C_{NObin}}\right) \times 100\% \quad (2)$$

$$NO_{2conversion} = \left(\frac{C_{NO_2in} - C_{NO_2light}}{C_{NO_2in}} - \frac{C_{NO_2bin} - C_{NO_2sb}}{C_{NO_2bin}}\right) \times 100\% \quad (3)$$

$$NO_{Xconversion} = \left(\frac{C_{NO_Xin} - C_{NO_Xlight}}{C_{NO_Xin}} - \frac{C_{NO_Xbin} - C_{NO_Xsb}}{C_{NO_Xbin}}\right) \times 100\% \quad (4)$$

The parameter meaning of equations 1,2, 3, and 4 are described in table 1.

The concentration of nitrates serves as evidence of a photocatalytic decrease of NO_x. Nitrates that accumulate on the pavement surface were measured by dissolving them in deionized water. Using the Japanese industrial standard (JIS TR Z 0018 “Photocatalytic materials--- air purification test procedure”), the nitrogen compound eluted from the test piece was calculated using the following formula (David et al. 2014):

$$Q_w = Q_{w1} + Q_{w2} = V_{w1}[(NO_3^-)_{w1}/62] + [(NO_3^-)_{w2}/62] \quad (5)$$

where Q_w = nitrogen compound eluted from the test piece (μmol); V_w = volume of collected washing (mL); NO_3^- = nitrate ion centration eluent from the test piece (mg/L); and W_1 and W_2 = the first and second DI washes, respectively.

Experimental testing: testing system and set-up

Experimental testing system

Photocatalytic degradation of NO_x was carried out using a continuous flow system that included a gas supply subsystem, photoreactor, and the analytic subsystem. NO_x, N_2, and humidified air were supplied in the gas supply subsystem. Humidified air was prepared by bubbling air through a gas wash bottle containing water. The desired water vapor level can be obtained by varying the flow rate of the humidified air stream. To obtain a stable NO_x concentration, NO_x is mixed with humidified air in a gas mixer. During the experiments, gas flow rates are controlled by calibrated flow meters. The photoreactor in the flow system is made of quartz glass in accordance with the American Material Test Association standard (ASTMD 5116-1990) and the Japanese industrial standard (photochemical catalysis material-air purification performance test method (Marwa et al. 2010)). To simulate on-road automobile exhaust, the photoreactor is divided into three parts (1) an inlet, (2) purification region and (3) outlet. The inlet section is nearly a cylinder; a fan controls the stream gas velocity. The purification section is rectangular, which simulates the road surface. Humidity and temperature sensors and a heater were installed in the photoreactor, and the photoreactor was irradiated by a simulation light source. Figure 4 shows the entire photoreactor structure. In the analytic subsystem, NO, NO_2, and NO_x concentration is measured by the analyzer.

Testing set-up

Photocatalytic activity rests: Previous studies on photocatalytic asphalt roads have shown that illumination by a light source is an essential condition for photodegradation of NO_x. Light source

illumination can cause the formation of electron–hole pairs on the photocatalytic asphalt road material and the electron–hole pair purified NO_x (Meng and Yan hua. 2010). In this study, we attempt to increase insight into the reduction of NO_x under photocatalytic asphalt road material by looking at the influence of the light source on the process.

During the serial experiment, the photocatalytic activity of N-doped TiO_2 photocatalytic asphalt road material was investigated by assessing the NO_x decomposition in the photoreactor. The experiment consisted of three steps.

Step 1: the sample was kept in the dark for 40 min, in order to achieve adsorption and desorption equilibrium of NO_x gas in the photoreactor.

Step 2: the light source was switched on. The range of the light wavelength is 330–420 nm, 430–530 nm (blue LED), 470–570 nm (green LED), and 590–680 nm (red LED).

Step 3: Photocatalytic characterizations of samples were shown using different NO_x concentration or decontamination rates. Direct measurement was used throughout the experiment.

Tests of application durability: In order to measure long term effects and examine decontamination durability, it is necessary to apply N-doped TiO_2 photocatalytic to asphalt road material to decontaminate exhaust from traffic in an outdoor environment. Vehicular activity and rainwash are major influencing factors in actual outdoor traffic environments.

A field and simulation test were adopted in order to predict the durability of the N-doped TiO_2 asphalt road material. In the field test, the test roads were washed once per week. At the same time, traffic volume, temperature, wind direction, wind speed, and humidity were recorded. During the test, the UV–vis spectroscopy (TU-1901) was used to determine absorbency of the gathered sample by N-(1-naphtyl)-cthylcncdiaminc dihydrochloride colori metric (Meng et al.

2014). The entire test was executed under nature flow conditions in the daytime and separate specimen exams lasted one hour. The field test location is shown in Figure 5.

Two separate simulation tests were conducted. First, in order to study the effect of vehicular activity, the Loaded-Wheel Tester was used to simulate loading and wear on the N-doped TiO_2 photocatalytic asphalt road surface (see Figure 6). The photocatalytic activities of samples that were subject to wear were investigated by evaluating the decomposition of NO_x in the photoreactor. The second test studied the rain wash effect. The samples were placed in to **a** traffic environment from June to August in Harbin, China. After this period a wash test was conducted. The samples were washed once a week and direct and indirect measurements were used to evaluate decontamination ability.

Results and discussion

Physical properties

TEM was executed to investigate the micrographs and dispersion of N-doped TiO_2 in the penetrant. Fig.6 shows that the micrographs of the N-doped TiO_2 are spherical and there is no significant shape change. The findings show that urea can help to hold or diminish the mean size and increase the homogeneity of the size distribution via the synthesis method, which has been described by other researchers (Hao-Hong et al. 2013). N-doped TiO_2 was also well dispersed in the penetrant as seen in Figure 8. An integrated method was used to ensure the dispersion effect of N-doped TiO_2 in the penetrant. It included three techniques. One technique used a silane coupling agent as a modifier, which should help N-doped TiO_2 to have good compatibility in the penetration process. Another technique involved choosing a magnetic stirrer for stirring the quantitatively modified

N-doped TiO_2. In the third tenchnique, an ultrasonoscope was used to disperse the mixing solution in order to reduce spontaneous reunion and flocculation.

The comprehensive dispersion method achieved a good dispersion effect for the following reasons: (1) The affinity between the nanoparticles and the solvent increased; meanwhile, it was easier to open the nano-granular equipment, reducing the dispersion time and energy consumption. (2) The strong turbulent motion of the liquid flow caused by the magnetic stirring broke and suspended the nano-particle and the ultrasonic agitation continued to disperse the nanoparticles into small particles, which led to a wide range of the solution region. (3) In the modifier component, one end of the active groups can be adsorbed on the surface of the crashed nanoparticles and the other end of the solvent formed adsorption layer, which produced electric charge repulsion, guaranteeing long dispersed suspension of the nanoparticles in the solvent, avoiding flocculation and ensuring the stability of the system.

Photocatalytic activity and purification mechanism

Figure. 9 shows the decontamination ability of the pure TiO_2 asphalt road material and N-doped TiO_2 asphalt road material, where the different wavelength lights (330–420 nm, 430–530 nm, 470–570 nm, and 590–680 nm) were irradiated to the samples. As seen in Figure 8, there was no loss of photoactivity in 330–420 nm wavelength lights (including in the UV section) on the pure TiO_2 asphalt road material and N-doped TiO_2 asphalt road material. Meanwhile, the N-doped TiO_2 asphalt road material had NO_x decontamination abilities of about 27.6%, 24.6%, 16.3%, and 13.8% under the irradiation of light wavelengths 330–420 nm, 430–530 nm, 470–570 nm, and 590–680 nm respectively. Further, on the N-doped TiO_2 asphalt road material under light irradiation, the NO decontamination ability was better than the NO_2 decontamination ability.

220 A number of results can be extracted from Figure 9.

221 (1) N-doped TiO_2 asphalt road materials have better photocatalytic activity under visible light

222 There are two potential reasons for this. First, it is well known that photocatalysts need light
223 illumination to trigger photocatalytic oxidation. Figure 8 shows that the N-doped TiO_2 asphalt
224 road material had better NO_x decontamination ability under a wavelength range of visible light.
225 The N-doped TiO_2 asphalt road material absorbed visible light to trigger photocatalytic oxidation.
226 Second, the behavior of the N-doped TiO_2 asphalt road material in the NO_x oxidation was also
227 associated with the active species (•OH and $O_2^{\bullet -}$) formed on the photocatalyst's surface
228 (Todorova et al. 2013). Excite electrons were required from the valence band to create electron
229 and hole pairs. Equation 6 (Shu et al. 2004) shows that energy decreases from irradiation for
230 exciting surface electrons and holes with increasing wavelength of the visible light. It indicated
231 that the band gap might be significantly narrowed by mechanical chemistry doping of nitrogen in
232 titanium, for instance 3.08 eV (Gagoa et al. 2012).

233 $$E_g = 1239.8/\lambda \quad (6)$$

234 where E_g is the band gap (eV) of the sample, λ (nm) is the wavelength of the onset of the
235 spectrum.

236 (2) N-doped TiO_2 asphalt road material had different photocatalytic activity under different
237 visible light wavelengths.

238 Figure 9 shows that the activity for the N-doped TiO_2 asphalt road material was clearly better
239 than the pure TiO_2 asphalt road material activity with increasing wavelengths. The findings were
240 attributed to the introduction of N in the TiO_2 lattice and the creation of extra electronic states in
241 the TiO_2 band gap (Kumar et al. 2011).

242 The N-doped TiO_2 samples possessed a two-step adsorption spectra. The first step may have
243 been related to the original titanium band structure and the second adsorption step (in the visible
244 light region) may have been related to the formation of additional electronic states during nitrogen
245 doping (Shu et al. 2008).

246 Figure 8 shows that decontamination of the NO_x ability of the N-doped TiO_2 asphalt road
247 material decreased with increasing wavelength of the light in. The rate of electron and hole pair
248 recombination was a key factor affecting the decontamination NO_x ability of N-doped TiO_2
249 asphalt road material (Yao-Hsuan et al.2011). Photoluminescence emission occurs when
250 wavelength photoenergy is absorbed to excite an electron from the valence band and then a longer
251 wavelength luminescence was emitted via recombination of the electron-hole pair (Chun-Hung et
252 al 2012). The greater the luminescence intensity was, the quicker the electron and hole
253 recombined. Therefore, high intensity of luminescence might result in low photocatalytic activity
254 (Yu et al., 2005). Therefore, the N-doped TiO_2 is capable of lowering the luminescence intensity
255 and guiding the higher photocatalytic activity under areas with shorter wavelengths.

256 (3) N-doped TiO_2 asphalt road material had a complicated photocatalytic mechanism.

257 By following the experimental results of the present study, we found that NO_2
258 decontamination ability was lower on the N-doped TiO_2 asphalt road material under light
259 irradiation. It has been shown that NO_2 was created in the photocatalytic purification process to
260 decrease NO_2decontamination ability. This may be explained by a tentative mechanism that is
261 proposed to explain photocatalytic oxidation of NO_x under visible light on the N-doped TiO_2
262 asphalt road surface, which is shown in Figure. 10.

263 It is widely recognized that photocatalytic oxidation can be divided into 3 core stages: first

the transfer of contaminants from bulk to the surface; second the adsorption on the catalyst surface and formation of reactive ions ; finally, degradation by the ions formed on the surface (Chuck et al.2 013). Based on Figure 10, a possible photocatalytic NO_x oxidation mechanism was proposed using equations (7)-(18).

N doping can build impurity states below the bottom of the conduction band of TiO_2 asphalt material, causing visible TiO_2 asphalt material to be activated by visible light (Hongqi et al.2011). N-doped TiO_2 asphalt road material was irradiated by appropriate light and energy, creating a hole and electron pair in the N-doped TiO_2 lattice, shown in equation (7).

$$\text{N-TiO}_2 + \text{visiblelight} \rightarrow h^+_{VB} + e^-_{CB} \quad (7)$$

During adsorption of the reactants onto the N-doped TiO_2 asphalt road material, the photogenerated hole in the conduction band will absorb water, oxygen, nitric oxide, and nitrogen dioxide in the air as described in equations (8) - (11).

$$\text{N-TiO}_2 + H_2O \Leftrightarrow \text{N-TiO}_2\text{-}H_2O \quad (8)$$

$$\text{N-TiO}_2 + O_2 \Leftrightarrow \text{N-TiO}_2\text{-}O_2 \quad (9)$$

$$\text{N-TiO}_2 + NO \Leftrightarrow \text{N-TiO}_2\text{-NO} \quad (10)$$

$$\text{N-TiO}_2 + NO_2 \Leftrightarrow \text{N-TiO}_2\text{-}NO_2 \quad (11)$$

In our previous work (Meng et al.2011), we found that adsorbed H_2O on the N-doped TiO_2 leads to the formation of a highly hydroxylated surface and also gives off hydrogen ions (H^+) and hydroxide ions (OH^-) by its dissociation. Then, H+ reacts with OH- to generate • OH.

Additionally, the photoinduced electron reacts with O_2, forming the superoxide anion (O_2^-) and O_2^- forms HO_2 • radicals with traces of water. Lastly, nitrogen species (NO, NO_2) in the air can be easily photocatalytically oxidized leading to HNO_3 by HO_2 • radicals on the N-doped TiO_2

asphalt road surface. The reaction is illustrated in equations (12) to (18).

$$H_2O \rightarrow H^+ + OH^- \quad (12)$$

$$h^+ + OH^- \rightarrow \bullet OH \quad (13)$$

$$e^- + O_2 \rightarrow O_2^- \quad (14)$$

$$HO_2\bullet + NO \rightarrow NO_2 + \bullet OH \quad (15)$$

$$NO + \bullet OH \rightarrow HNO_2 \quad (16)$$

$$HNO_2 + \bullet OH \rightarrow NO_2 + H_2O \quad (17)$$

$$NO_2 + \bullet OH \rightarrow HNO_3 \quad (18)$$

Durability Analysis

Figure. 11 shows the downward trend, over consecutive months, of the NO_x decontamination ability on the N-doped TiO_2 asphalt road. In order to predict the durability of the N-doped TiO_2 asphalt road, we hypothesized that the N-doped TiO_2 asphalt road will actively degrade when the NO_x decontamination rate is less 5%. An exponential regression model was used with the observed data that was obtained in the field test (see Figure 11). The model was y=32.01e^(-0.145x), with 95% confidence. Results from the model showed that active degradation of the asphalt pavement lasted for a period of about 13 months. The photocatalytic efficiency defeat was due to the wear from traffic and the rain wash. Wear and wash simulation tests were completed in order to analyze these reasons.

In the wear simulation test, as seen in table 2, the data showed s decrease in NO_x decontamination ability after wearing. However, the decrease was small under a certain scope, such as in 8000 cycles where the wheel applied a load of 600 N for every cycle. But when the cycle increased (exceeding 8000 cycles), the degree of decrease in the NO_x decontamination

ability increased. This had two possible causes: (1) the samples kept higher NO_x removal efficiencies after wear, and, (2) N-doped TiO_2 was retained on the asphalt road surface and interior after wearing, which may be proven by figure 12. This may be attributed to the research team's use of infiltration liquid with N-doped TiO_2 and the permeability loading method. The infiltration liquid had a special lipophilic penetration ability. When the infiltration liquid is sprayed on the road surface, the nano-material (N-doped TiO_2) can be guaranteed to gradually infiltrate the road surface under the action of the penetrating agent molecular power. Subsequently, with the growth of the concentration of the asphalt pavement surface infiltration liquid and the dual influences of the concentration gradient and porous open graded pavement, N-doped TiO_2 penetrates along the open graded asphalt pavement pore to the core under the action of capillary force and gravity. During the penetration process, when the N-doped TiO_2 molecules are near the asphalt mixture solid surface, N-doped TiO_2 molecules can adsorb on the solid surface in order to achieve the load. This is because of the electric dipole moment and is possible because of the help of the Van Der Waals force. However, when the cycle increases, the loss of weight in the samples also increases. Surface wearing and particle loss may be associated with the loss of N-doped TiO_2 particles, which is shown in figure 13. NO_x decontamination ability decreases as the cycles increase.

Table 2 presents the average NO_x decontamination ability for both the original and the washed samples. The table shows that washing the samples results in reduction in the NO_x removal efficiency and this decline was aggravated with time. This indicates time dependency, which will result in a decrease of the NO_x removal efficiency. There are many reasons for this. First, the decrease can be clarified by referencing the NO_x purification mechanisms found in section 3.2 of this paper. HNO_3 should be speedily produced and accumulated on the top of the

N-doped TiO_2 asphalt road surface, and this could inhibit the photocatalytic reactions by building a physical fence. Next, regeneration of the purification ability has proven that washing is a better way to keep the NO_x decontamination ability for N-doped TiO_2 asphalt road material. During washing, the HNO_3 was easily removed from the catalyst surface (as indirect measurement results); it can be argued this may contribute to catalyst regeneration. Water can also, through rehydration, replenish the consumed hydroxyl radicals; therefore, it is able to maintain the photocatalyst activity (Meng et al.2011). However, the continuing decrease of the NO_x removal efficiency also indicated that washing did not totally recover the active N-doped TiO_2 asphalt road material. That may be due to the adsorption of indissolvable materials, such as lipids, on the photocatalyst receptor sites of N-doped TiO_2 asphalt road material. Adsorption of NO_x occurred on the N-doped TiO_2 asphalt road.

Summary and future work

N-doped TiO_2 powders were successfully prepared by sol–gel methods with urea. The modified procedures did not change the crystalline structure or the morphology of the N-doped TiO_2 as compared with initial sol–gel TiO_2. TEM analysis revealed that N-doped TiO_2 powders could be well dispersed in asphalt penetrants. Based on the penetrant, N-doped TiO_2 asphalt road materials were successfully prepared using spray methods.

Meanwhile, the N-doped TiO_2 asphalt road materials presented higher activity on NO_x removal than pure TiO_2 asphalt road materials under the irradiation of visible light. The outcome was ascribed to the photocatalytic mechanism. As described by this mechanism, the nitrogen species onto The iO_2 interfaces decreased the absorption band gap energy in the visible light and hindered the electron hole recombination, which helped to improve oxidation of nitrogen oxides.

The durability of N-doped TiO_2 asphalt road materials was evaluated through field and simulation testing. Results suggested that the durability of N-doped TiO_2 asphalt road materials spanned a period of approximately 13 months. The results demonstrated that the TiO_2 nitrogen doping approach would provide a worthy channel for photocatalytic asphalt road materials of highly visible light induced photocatalytic activity for the practical decontamination NO_x application in the medium-term.

Because the application of N-doped TiO_2 asphalt road materials in demonstrating vehicle emissions is still a relatively new field of study, more research should be conducted prior to field application. Our research team plans to evaluate the potential pollution of nitrates created by the photocatalytic processing in land through plant experiments. We will also attempt to build an evaluation system for N-doped TiO_2 asphalt road materials application for demonstrating vehicle emissions.

Acknowledgments

The authors gratefully acknowledge the funding support by the National Natural Science Foundation of China (Grant No. 31470611, 51378096), Research Fund for the Doctoral Program of Higher Education of China (Grant No. 20120062120011) ,the Natural Science Foundation of Heilongjiang Province (Grant No. E2015055) and the Fundamental Research Funds for the Central Universities (Grant No. 2572014CB16), respectively.

References

Giacomo Barolo, Stefano Livraghi, Mario Chiesa, Maria Cristina Paganini, and Elio Giamello. (2012). “Mechanism of the Photoactivity under Visible Light of N‐Doped Titanium

374 Dioxide. Charge Carriers Migration in Irradiated N‑TiO_2 Investigated by Electron
375 Paramagnetic Resonance. ” The Journal of Physical Chemistry C 116:20887−20894.
376 Hao-Hong Chen, Fang Lei, Jing-Tai Zhao, Ying Shi ,Jian-Jun Xie. (2013). “Preparation and
377 photovoltaic properties of N-doped TiO_2 nanocrystals in vacuum.” Journal of Materials
378 Research 28:468-47.
379 Meng Chen, Jiang-Wei Chu. (2011). “NO_x photocatalytic degradation on active concrete road
380 surface d from experiment to real-scale application.” Journal of Cleaner Production 19:
381 1266-1272.
382 Meng Chen, Li sheng Jin, Yanhua Liu, Xiurong Guo, Jiangwei Chu. (2014). “Decomposition of
383 NO in automobile exhaust by plasma-photocatalysis synergy.” Environmental Science and
384 Pollution Research 21:1242–1247.
385 Meng Chen, Yan hua Liu. (2010). “NO_x removal from vehicle emissions by functionality surface
386 of asphalt road.” Journal of Hazardous Materials 174:375–379.
387 Poon CS, Cheung E (2006). “NO removal efficiency of photocatalytic paving blocks prepared
388 with recycled materials.” Construction and Building Materials 21: 1746–53.
389 Husken G, Hunger M, Brouwers H. (2007). “Comparative study on cementitious products
390 containing titanium dioxide as photo-catalyst. ” In: Baglioni P, Cassar L, eds. RILEM Int.
391 Symp. On Photocatalysis. Environment and Construction Materials. Italy 147–54.
392 G.L.Guerrini, E.Peccati. (2007). “Photocatalytic cementitious roads for depollution, in: P.Baglioni,
393 L. Cassar (Eds.), Proceedings international RILEM symposium on photocatalysis.”
394 Environment and construction materials-TDP 2007, RILEM Publications, Bagneux
395 187–194.

Ishihara, H., Koga, H., Kitaoka, T., Wariishi, H., Tomoda, A., Suzuki, R. (2010). “Paper-structured catalyst for catalytic NO_x removal from combustion exhaust gas. ” Chemical Engineering Journal 65: 208–213.

Marwa Hassan, Louay N. Mohammad, Somayeh Asadi. (2013). “Sustainable Photocatalytic Asphalt Pavements for Mitigation of Nitrogen Oxide and Sulfur Dioxide Vehicle Emissions.” Journal of Materials in Civil Engineering 3:365-371.

Chun-Hung Huanga, I-Kai Wanga, Yu-Ming Linb, Yao-Hsuan Tsengc, Chun-Mei Lud. (2010). “Visible light photocatalytic degradation of nitric oxides on PtOx-modified TiO_2 via sol–gel and impregnation method.” Journal of Molecular Catalysis A: Chemical 316:163–170.

Chun-Hung Huang, Yu-Ming Lin, I-Kai Wang, and Chun-Mei Lu. (2012). “Photocatalytic Activity and Characterization of Carbon-Modified Titania for Visible-Light-Active Photodegradation of Nitrogen Oxides.” International Journal of Photoenergy 2012: 1-13.

Venturini, L., and Bacchi, M. (2009). “Research, design, and development of a photocatalytic asphalt pavement. ”Proc., 2nd Int. Conf. on Environmentally Friendly Roads, Road and Bridge Research Institute, Warsaw, Poland 1–16.

Marwa M.Hassan, Heather Dylla, Louay N.Mohammad, Tyson Rupnow. (2010). “Evaluation of the durability of titanium dioxide photocatalyst coating for concrete pavement.” Construction and Building Materials 24:1456–1461.

Todorova.N, T.Vaimakis, D. Petrakis, S. Hishita, N. Boukos, T. Giannakopoulou, M. Giannouri,S. Antiohos, D. Papageorgiou, E. Chaniotakis, C. Trapalis. (2013). “N and N,S-doped TiO_2 photocatalysts and their activity in NOx oxidation. ” Catalysis Today 209:41–46.

418 Tarek Mohamed Naser, Isao Kanda, Toshimasa Ohara, Kazuhiko Sakamoto, Shinji Kobayashi,
419 Hiroshi Nitta, Taro Nataami. (2009). "Analysis of traffic-related NO_x and EC
420 concentrations at various distances from major roads in Japan." Atmospheric Environment
421 43: 2379–2390.

422 David Osborn, Marwa Hassan, Somayeh Asadi, John R. White. (2014). "Durability Quantification
423 of TiO_2 Surface Coating on Concrete and Asphalt Pavements." Journal of Materials in
424 Civil Engineering 26:331-337.

425 Gagoa.R, A. Redondo-Cubero b, M. Vinnichenkoc, J. Lehmannc, F. Munnikc, F.J. Palomares.
426 (2012). "Spectroscopic evidence of NO_x formation and band-gap narrowing in N-doped
427 TiO_2 films grown by pulsed magnetron sputtering." Materials Chemistry and Physics
428 136:729-736.

429 Shinri Sato. (1986). "Photocatalytic activity of NO_x-doped TiO_2 in the visible light region."
430 Chemical Physics Letters 123:126-128.

431 Kumar.S.C, L.G. Devi. (2011). "Review on modified TiO_2 photocatalysis under UV/visible light:
432 selected results and related mechanisms on interfacial charge carrier transfer dynamics."
433 Journal of Physical Chemistry A 115:13211–13241.

434 Hongqi Sun, Ruh Ullah, Siewhui Chong, Hua Ming Ang, Moses O. Tadé, Shaobin Wang. (2011).
435 "Room-light-induced indoor air purification using an efficient Pt/N-TiO_2 photocatalyst."
436 Applied Catalysis B: Environmental 108–109:127–133.

437 Yao-Hsuan Tseng, Chien-Hung Kuo. (2011). "Photocatalytic degradation of dye and NO_x using
438 visible-light-responsive carbon-containing TiO_2." Catalysis Today 174:114–120.

439 Yu.Y, J. C. Yu, J. G. Yu. (2005). "Enhancement of photocatalytic activity of mesoporous TiO_2 by

using carbon nanotubes.” Applied Catalysis A289: 186–196.

Shu Yin, Bin Liu, Peilin Zhang, Takeshi Morikawa, Ken-ichi Yamanaka, and Tsugio Sato. (2008). “Photocatalytic Oxidation of NO_x under Visible LED Light Irradiation over Nitrogen-Doped Titania Particles with Iron or Platinum Loading.” Joural of Physical Chemistry. C 112: 12425–12431.

Shu Yin, Hiroshi Yamaki, Qiwu Zhang, Masakazu Komatsu, Jinshu Wang,Qing Tang, Fumio Saito, Tsugio Sato. (2004). “Mechanochemical synthesis of nitrogen-doped titania and its visible light induced NO_x destruction ability.” Solid State Ionics 172:205–209.

Chuck W.F. Yu, Jeong Tai Kim. (2013). “Photocatalytic Oxidation for Maintenance of Indoor Environmental Quality.” Indoor and Built Environment 22: 139-51.

458 Table 1 parameter nomenclature

Parameter	Meaning
$NO_{conversion}$ (%)	effective purifying rate of NO
$NO_{2conversion}$ (%)	effective purifying rate of NO_2
$NO_{xconversion}$ (%)	effective purifying rate of NO_x
C_{NOin} (mg/m^3)	the initial steady-state NO concentration (before turn on the light source)
C_{NO2in} (mg/m^3)	the initial steady-state NO_2 concentration (before turn on the light source)
C_{NOxin} (mg/m^3)	the initial steady-state NO_x concentration (before turn on the light source)
$C_{NOlight}$ (mg/m^3)	the NO concentration during irradiation phase
$C_{NO2light}$ (mg/m^3)	the NO_2 concentration during irradiation phase
$C_{NOxlight}$ (mg/m^3)	the NO_x concentration during irradiation phase
C_{NObin} (mg/m^3)	the initial steady state NO concentration
C_{NO2bin} (mg/m^3)	the initial steady state NO_2 concentration
C_{NOxbin} (mg/m^3)	the initial steady state NO_x concentration
C_{NOsb} (mg/m^3)	the NO concentration at the end of the blank experiment(without irradiation)
C_{NO2sb} (mg/m^3)	the NO_2 concentration at the end of the blank experiment(without irradiation)
C_{NOxsb} (mg/m^3)	the NO_x concentration at the end of the blank experiment(without irradiation)

459

460

461

462

463

464

465 Table 2 Degradation effect of wear and wash

$DeNO_x$ ability	Number of wear (cycle)					Number of wash (time)				
	0	4000	8000	12000	16000	0	2	4	6	8
Direct measurement-purification rate (%)	36.4	34.8	32.1	28.1	22.3	36.4	34.2	32.8	29.3	24.6
Indirect measurement- . nitrate concentrations s in the sample (mg/L)	8.3	8.1	7.2	5.5	3.8	8.3	7.9	7.3	6.1	4.1

466

Fig 1. Pure TiO_2 and N-doped TiO_2

Fig 2. Asphalt road material sample before spray

Fig 3. N-doped TiO_2 asphalt road material sample

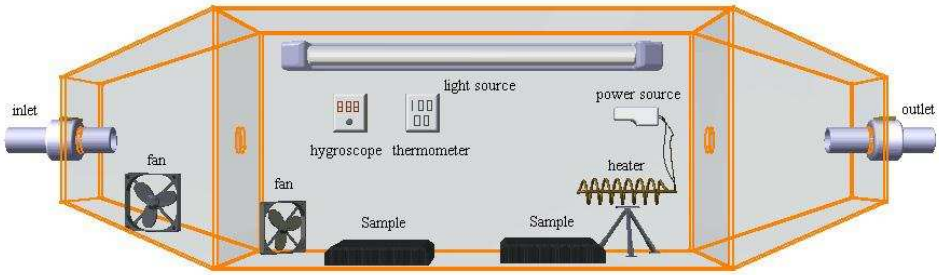

Fig 4. Structure of photoreactor

Fig 5. Spot of field test

Fig 6. Simulation test on vehicular activity effect

Figure

Click here to download Figure Fig 7. Micrographs of the N-doped TiO2.pdf

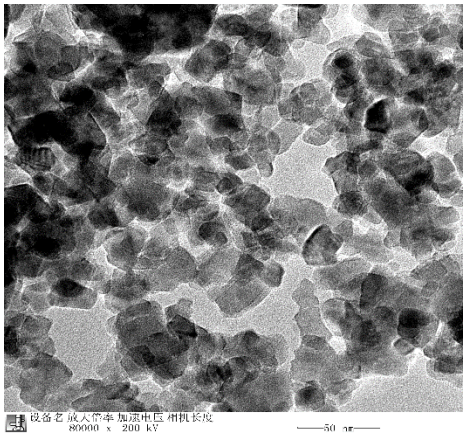

Fig 7. Micrographs of the N-doped TiO_2

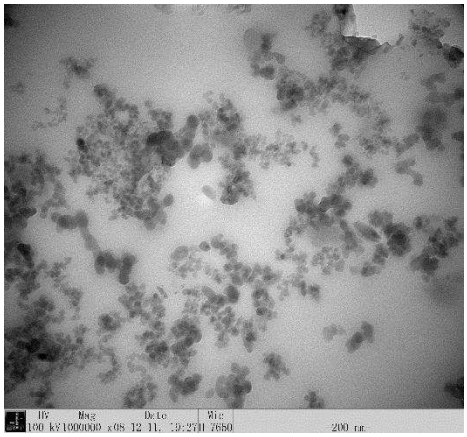

Fig 8. Dispersion effect of N-doped TiO_2 in penetrant

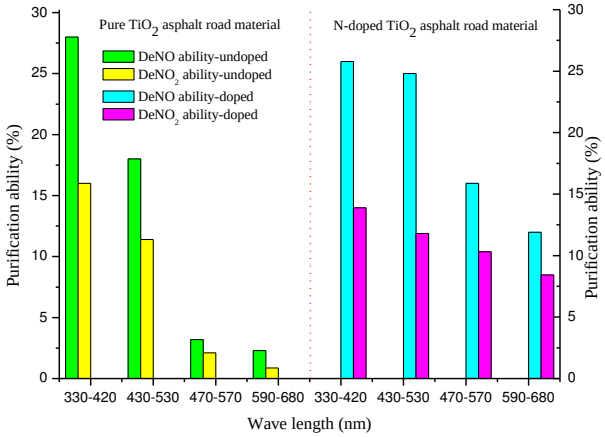

Fig 9 Comparison of the photocatalytic activity of undoped, N-doped TiO_2 asphalt road material under UV and visible light

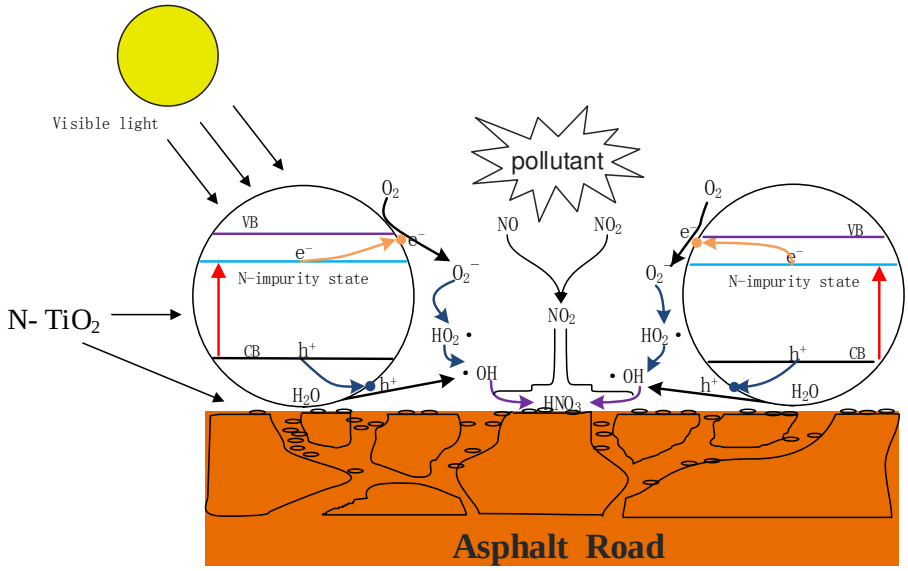

Fig 10. Schematic illustration of photocatalytic process on N-doped TiO_2 asphalt road material under visible light

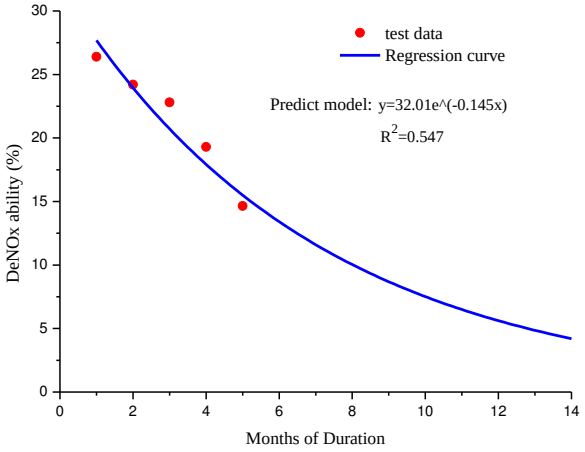

Fig 11 Illustration of durability of N-doped TiO_2 asphalt road

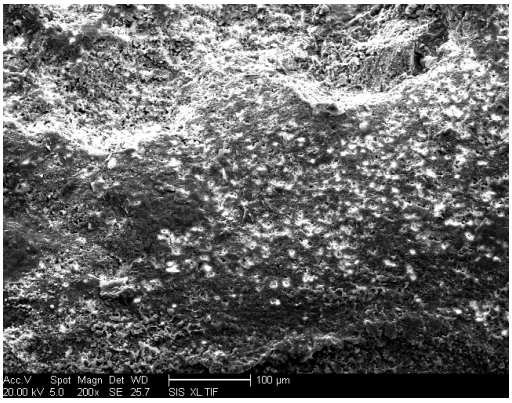

Fig 12 SEM image of road surface after wearing

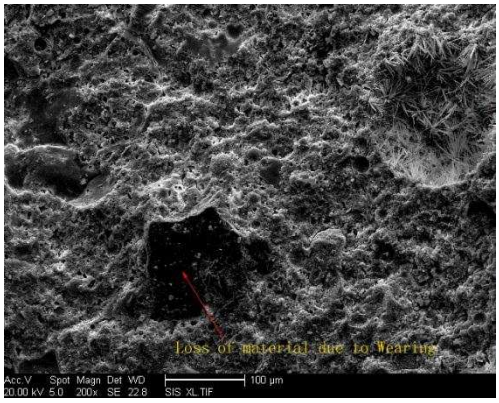

Fig 13 SEM on loss of N-doped TiO_2 due to wearing

Figure Caption List